

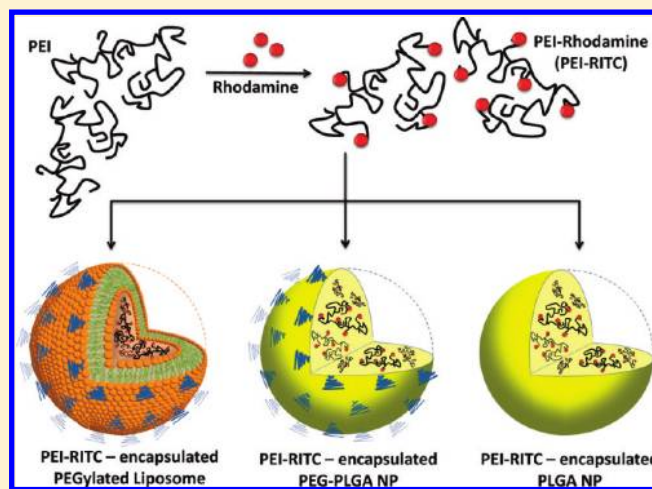
Kinetically Controlled Cellular Interactions of Polymer–Polymer and Polymer–Liposome Nanohybrid Systems

 Suhair Sunoqrot,[†] Jin Woo Bae,[†] Su-Eon Jin,[†] Ryan M. Pearson,[†] Ying Liu,^{†,‡} and Seungpyo Hong^{*,†,§}

 Departments of [†]Biopharmaceutical Sciences, [‡]Chemical Engineering, and [§]Bioengineering, University of Illinois at Chicago, Chicago, Illinois, United States

Supporting Information

ABSTRACT: Although bioactive polymers such as cationic polymers have demonstrated potential as drug carriers and nonviral gene delivery vectors, high toxicity and uncontrolled, instantaneous cellular interactions of those vectors have hindered the successful implementation *In Vivo*. Fine control over the cellular interactions of a potential drug/gene delivery vector would be thus desirable. Herein, we have designed nanohybrid systems (100–150 nm in diameter) that combine the polycations with protective outer layers consisting of biodegradable polymeric nanoparticles (NPs) or liposomes. A commonly used polycation polyethylenimine (PEI) was employed after conjugation with rhodamine (RITC). The PEI–RITC conjugates were then encapsulated into (i) polymeric NPs made of either poly(lactide-co-glycolide) (PLGA) or poly(ethylene glycol)-*b*-poly(lactide-co-glycolide) (PEG-PLGA); or (ii) PEGylated liposomes, resulting in three nanohybrid systems. Through the nanohybridization, both cellular uptake and cytotoxicity of the nanohybrids were kinetically controlled. The cytotoxicity assay using MCF-7 cells revealed that liposome-based nanohybrids exhibited the least toxicity, followed by PEG-PLGA- and PLGA-based NPs after 24 h incubation. The different kinetics of cellular uptake was also observed, the liposome-based systems being the fastest and PLGA-based systems being the slowest. The results present a potential delivery platform with enhanced control over its biological interaction kinetics and passive targeting capability through size control.



INTRODUCTION

Multifunctional macromolecules have demonstrated great potential as drug delivery vectors.^{1,2} In particular, polycationic polymers have been widely explored for many biomedical applications, including gene delivery.³ One of the most commonly used cationic polymers is polyethylenimine (PEI), which has been mainly used as a nonviral gene delivery vector, as it is capable of protecting DNA from lysosomal degradation and promoting endosomal escape.^{4–7} Another characteristic of PEI and other polycations, such as poly(lysine) and poly(amidoamine) (PAMAM) dendrimers is that they spontaneously interact with biological membranes.^{8,9} Although the mechanism is not yet completely understood, this facilitates their cellular internalization without the need for ligands for receptor-mediated endocytosis or other internalization routes. However, toxicity issues related to the strong cationic surface charge have hindered clinical translation of the polycations in drug delivery, largely due to the lack of kinetic control over nonspecific electrostatic interactions with blood components and rapid clearance by the reticuloendothelial system (RES).¹⁰ Therefore, a better understanding on the cellular interaction kinetics of

polycation-based drug delivery systems is required, which would eventually lead to fine control over their toxicity as well as cellular internalization.

As most of the currently available anticancer treatment agents frequently accompany severe side effects through high toxicity to normal cells and tissues, it is highly desirable to home the drug delivery system to the tissue of interest. The passive targeting strategy using nanotechnology has proven to be efficient in reducing the toxic side effects, thereby increasing the therapeutic index of anticancer agents.^{11–13} Passive targeting utilizes the enhanced permeability and retention (EPR) effect that is defined by leaky vasculature and poor lymphatic drainage around tumors, resulting in the accumulation of the nanoscale delivery system at the tumor site. In order to take advantage of the EPR effect, a nanoscale delivery system needs to be in the range of 50–200 nm, which can be achieved using well-established manufacturing techniques.^{14,15}

Received: November 5, 2010

Revised: January 26, 2011

Published: February 23, 2011

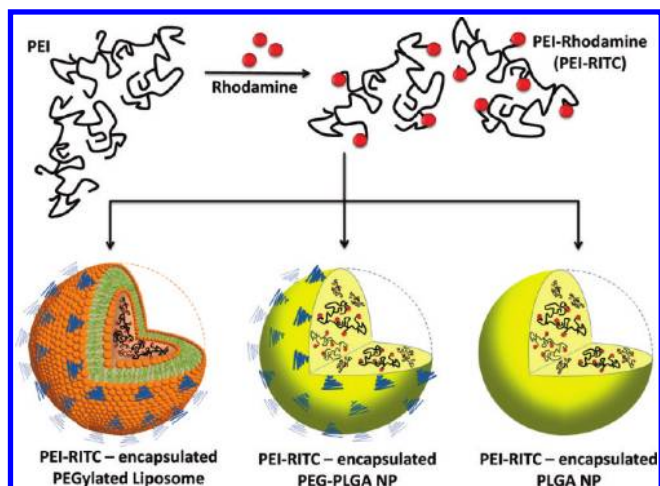


Figure 1. Schematic diagram of preparation of the three nanohybrid systems used in this study.

As the first step in achieving kinetic control over the toxicity and cellular interactions of polycations, we have designed novel hybrid nanomaterials that combine functionalized PEI with relatively bioinert, biodegradable polymer-based nanoparticles (NPs) and PEGylated liposomes. The design rationale of our nanohybrid systems is for a temporal control over interactions with cells, i.e., achieving passive targeting first by controlling the size of the nanohybrid materials and subsequent control over the kinetics of cellular interactions upon the release of PEI. The objectives of this study were to (i) encapsulate functionalized PEI into polymeric NPs or liposomes at a controlled size range of ~ 100 nm and (ii) control the cellular uptake and cytotoxicity of PEI, depending upon the physical properties (such as biodegradability and structural stability) of the encapsulating materials as the protective outer layers. We have prepared three types of the nanohybrid systems that encapsulate PEI-rhodamine (PEI-RITC) conjugates, as outlined in Figure 1. For the nanohybrid polymeric NPs, PEI was encapsulated into either poly(lactide-co-glycolide) (PLGA) or poly(ethylene glycol)-*b*-poly(lactide-co-glycolide) (PEG-PLGA) using the double emulsion method. These systems were compared to PEGylated liposomes of mixed phospholipid composition, where PEI was encapsulated using the film rehydration method followed by extrusion.

Here, we report three nanohybrid systems where a multifunctional polymer such as PEI is successfully encapsulated into either polymeric NPs or liposomes. Although similar hybrid systems that incorporate PEI into liposomes or biodegradable NPs have been reported in the literature,^{16–18} no attempt has been made to compare them for the purpose of understanding the kinetics of their interactions with cells. By comparing the release profiles, cytotoxicity, and cellular uptake of the three PEI-based nanohybrids, we demonstrate that fine control over release and cellular uptake kinetics of the nanohybrids can be achieved depending on the type of the outer layers. Our results provide an important guideline in designing a drug delivery platform with tunable cellular interactions and cytotoxicity kinetics.

EXPERIMENTAL SECTION

Materials. Branched PEI (M_n 10,000), PLGA (50:50, M_w 40,000–75,000), poly(vinyl alcohol) (PVA, 87–89%

hydrolyzed, M_w 13,000–23,000), rhodamine B isothiocyanate (RITC, mixed isomers), dichloromethane (DCM), pyridine, *p*-nitrophenyl chloroformate (*p*-NPC), triethylamine (TEA), diethyl ether, and cholesterol were all obtained from Sigma-Aldrich (St. Louis, MO). Amine-terminated methoxy PEG (mPEG-NH₂) (M_w 5,000) was obtained from Nektar (Huntsville, AL). 1,2-Distearoyl-*sn*-glycero-3-phosphoethanolamine-*N*-mPEG-2000 (DSPE-PEG 2000), 1,2-distearoyl-*sn*-glycero-3-phosphocholine (DSPC), and 1,2-dioleoyl-*sn*-glycero-3-phospho-(1'-*rac*-glycerol) sodium salt (DOPG) were purchased from Avanti Polar Lipids Inc. (Alabaster, AL). All other chemicals used in this study were purchased from Sigma-Aldrich unless specified otherwise.

Preparation and Characterization of PEI-RITC conjugates. PEI was fluorescently labeled by conjugation with RITC using a method similar to that described earlier.⁹ RITC (5.4 mg, 1.0×10^{-5} mol) dissolved in 1 mL of deionized distilled water (ddH₂O) was added to PEI (20.0 mg, 2.0×10^{-6} mol) dissolved in 4 mL of ddH₂O. The pH of the mixture was adjusted to 9.0 using 1.0 N hydrochloric acid (HCl), followed by vigorous mixing at room temperature (RT) for 24 h. Unreacted RITC was removed using membrane dialysis (Spectra/Por dialysis membrane, MWCO 3,500, Spectrum Laboratories Inc., Rancho Dominguez, CA) in 3 L of phosphate buffered saline (PBS) for 2 days, changing the buffer every 12 h, followed by dialysis in ddH₂O for 2 days, changing the water every 12 h. The purified PEI-RITC conjugates were lyophilized over 2 days using a Labconco FreeZone 4.5 system (Kansas City, MO) and stored at -20 °C.

UV/Vis Spectroscopy. A series of RITC solutions in ddH₂O (6.3, 12.5, 25.0, 37.5, and 50.0 $\mu\text{g/mL}$) were prepared and used as standards to calculate the RITC content of the conjugates in subsequent measurements. PEI-RITC conjugates were dissolved in ddH₂O at a concentration of 100 $\mu\text{g/mL}$. UV spectra were recorded against ddH₂O using a DU800 UV/vis Spectrophotometer (Beckman Coulter, CA). A standard curve of RITC absorbance versus concentration was constructed, and the concentration of RITC in the PEI-RITC solution was calculated on the basis of Beer's law. The number of RITC molecules per PEI chain was determined on the basis of the amount of RITC in the PEI-RITC solution.

Synthesis and Characterization of the PEG-PLGA Copolymer. The PEG-PLGA block copolymer used in this study was synthesized from mPEG-NH₂ and PLGA using a method similar to that described earlier.¹⁹ Five hundred milligrams of PLGA (1.3×10^{-5} mol) was dissolved in 8 mL of DCM, to which 5.1 μL (6.3×10^{-5} mol) of pyridine was added. *p*-NPC (12.6 mg, 6.3×10^{-5} mol) was dissolved in 1 mL of DCM and then added dropwise to the PLGA and pyridine solution under vigorous stirring, and the reaction was carried out at RT for 24 h. The reaction product (*p*-NP-PLGA) was then precipitated using ice-cold diethyl ether and vacuum filtered. Next, *p*-NP-PLGA (400 mg, 1.0×10^{-5} mol) was dissolved in 8 mL of DCM. mPEG-NH₂ (93.8 mg, 1.9×10^{-5} mol) was dissolved in 3 mL of DCM, to which 7 μL (5.0×10^{-5} mol) of TEA was added. The mPEG-NH₂ and TEA solution was then added dropwise to the *p*-NP-PLGA solution under vigorous stirring, and the reaction was carried out at RT for 24 h. The final product (PEG-PLGA) was precipitated using ice-cold diethyl ether and vacuum filtered. PEG-PLGA was characterized using ¹H NMR in CDCl₃ using a 400 MHz Bruker DPX-400 spectrometer (Bruker BioSpin Corp., Billerica, MA).

Encapsulation of PEI–RITC Conjugates into Polymeric NPs. PLGA and PEG-PLGA NPs were prepared using a double emulsion method as described previously.²⁰ Briefly, 20 mg of either PLGA or PEG-PLGA was dissolved in 1 mL of DCM. PEI–RITC was dissolved in ddH₂O at a concentration of 1 mg/mL, and 100 μ L of the solution was added to either PLGA or PEG-PLGA solution in DCM. The mixture was sonicated for 1 min using a Misonix XL Ultrasonic Processor (100% duty cycle, 475 W, 1/8" tip, QSonica, LLC, Newtown, CT). Two milliliters of 3% PVA solution in ddH₂O was then added to the mixture, followed by sonication for 1 min at 100% duty cycle. The double emulsion was then poured into 20 mL of 0.3% PVA in ddH₂O, and vigorously stirred at RT for 24 h to evaporate DCM. The resulting aqueous solution was transferred to Nalgene high-speed centrifuge tubes (Fisher Scientific, Pittsburgh, PA). PVA and unencapsulated PEI–RITC were removed by ultracentrifugation at 20,000 rpm for 30 min using a Beckman Avanti J25 Centrifuge (Beckman Coulter, Brea, CA). After washing the NPs five times with ddH₂O, the pellet was resuspended in ddH₂O, lyophilized over 2 days, and stored at -20°C .

Characterization of the PEI–RITC-Encapsulated Polymeric NPs. Particle size (diameter, nm) and surface charge (zeta potential, mV) of the NP-based nanohybrids were obtained from three repeat measurements by quasi-elastic laser light scattering using a Nicomp 380 Zeta Potential/Particle Sizer (Particle Sizing Systems, Santa Barbara, CA). The nanohybrid particles were suspended in ddH₂O at a concentration of 100 μ g/mL, filtered through a 0.45 μ m syringe filter, and briefly vortexed prior to each measurement. Loading was defined as the PEI–RITC content of the NP-based nanohybrids. Five milligrams of NP-based nanohybrids were completely dissolved in 1 mL of 0.5 M NaOH, followed by filtration through a 0.45 μ m syringe filter. The fluorescence intensity from the filtrates containing PEI–RITC was then measured using a SpectraMAX GeminiXS microplate spectrofluorometer (Molecular Devices, Sunnyvale, CA). The amount of PEI–RITC released was determined from a standard curve of PEI–RITC fluorescence versus concentration in 0.5 M NaOH. Loading was expressed as μ g PEI–RITC/mg PLGA or PEG-PLGA. Loading efficiency was defined as the ratio of the actual loading obtained to the theoretical loading (amount of PEI–RITC added divided by the mass of PLGA or PEG-PLGA used in each formulation).

Scanning Electron Microscopy (SEM). The surface morphology of PLGA and PEG-PLGA NPs was examined using a JEOL-JSM 6320F field emission microscope (JEOL USA, Peabody, MA). Freeze-dried NP samples were placed onto a carbon adhesive strip mounted on an aluminum stub. Samples were sputter-coated with Pt/Pd at a coating thickness of 6 nm (Polaron ES100 sputter coater system, Polaron, UK) and then visualized at an accelerating voltage of 5.0 mV and 8.0 mm working distance.

Encapsulation of PEI–RITC Conjugates into Liposomes. Unilamellar liposomes were prepared using a film hydration method followed by extrusion as described previously.¹⁶ Briefly, DOPG (5.0 mg, 6.3×10^{-6} mol), DSPC (4.9 mg, 6.2×10^{-6} mol), cholesterol (2.4 mg, 6.2×10^{-6} mol), and DSPE-PEG 2000 (1.8 mg, 6.3×10^{-7} mol) were dissolved in 5 mL of DCM in a round-bottom flask. The flask was connected to a rotary evaporator (Rotavapor RII, Buchi, Switzerland) at 50°C for 1 h to evaporate DCM until completely dried. The dried lipid film was hydrated in 1 mL of 0.1 mg/mL PEI–RITC solution in ddH₂O, followed by vortexing for 15 min to form multilamellar

liposomes. Multilamellar liposomes were sonicated in a bath sonicator for 30 min and then extruded 20 times through a polycarbonate membrane of 100 nm pore size using a Lipofast Pneumatic extruder (Avestin Inc., Ottawa, Canada). The resulting unilamellar liposome suspension was centrifuged at 20,000 rpm for 1 h to remove residual PEI–RITC. The pellet was resuspended in 1 mL of 5% sucrose, lyophilized over 2 days, and stored at -20°C .

Characterization of the PEI–RITC-Encapsulated Liposomes. Particle size (diameter, nm) and surface charge (zeta potential, mV) were measured using the same method described for polymeric NPs. Loading was determined by dissolving 10 mg of lyophilized liposomes in 1 mL of 0.1% Triton X-100, followed by filtration through a 0.45 μ m syringe filter and measuring the fluorescence of the filtrate. The amount of PEI–RITC released was determined from a standard curve of PEI–RITC fluorescence versus concentration in 0.1% Triton X-100. Loading was expressed as μ g PEI–RITC/mg lipids. Loading efficiency was calculated from the ratio of the actual measured loading to the theoretical loading (amount of PEI–RITC added divided by the mass of lipids and sucrose used in the formulation).

Transmission Electron Microscopy (TEM). Size and shape of liposomal nanohybrids was examined using TEM. Liposomes were dissolved in ddH₂O at a concentration of 1 mg/mL. One drop of the solution was then placed on a 300-mesh copper grid and left to dry overnight, followed by negative staining with 2% phosphotungstic acid (PTA). TEM images were acquired using a JEOL JEM 1220 (JEOL USA) at an accelerating voltage of 80 kV.

Release Kinetics Study of PEI–RITC-Encapsulated Nanohybrids. Five milligrams of each nanohybrid in microcentrifuge tubes were dispersed in 1 mL of PBS (pH 7.4) or acetate buffer (pH 4.0) in triplicate, and the solutions were placed in a shaking water bath (37°C , 100 rpm). At designated time points (30 min, 1 h, 2, 4, 6, 8, 10, 12, and 24 h; every 2 days thereafter), solutions were centrifuged at 20,000 rpm for 5 min, and the supernatants were collected. The nanohybrid systems were then redispersed in fresh PBS or acetate buffer and placed back in the water bath. The fluorescence of the supernatants was measured, and the cumulative amount of PEI–RITC released over time was determined from a standard curve of PEI–RITC fluorescence versus concentration in either PBS or acetate buffer.

Cytotoxicity of PEI–RITC-Encapsulated Nanohybrids. The MCF-7 cell line was obtained from ATCC (Manassas, VA) and grown continuously as a monolayer in GIBCO Dulbecco's modified Eagle's medium (DMEM, Invitrogen Corporation, Carlsbad, CA) in a humidified incubator at 37°C and 5% CO₂. DMEM was supplemented with penicillin (100 units/mL), streptomycin (100 mg/mL), and 10% heat-inactivated fetal bovine serum (FBS) (Invitrogen Corporation, Carlsbad, CA) before use. For the assay, MCF-7 cells were seeded in 96-well plates at a density of 2×10^4 cells/well and grown in DMEM for 24 h. Cells ($n = 4$) were then treated with PEI–RITC or nanohybrid systems (PEI–RITC encapsulated liposomes, PEG-PLGA NPs, and PLGA NPs) at 4 PEI–RITC concentrations (1, 5, 10, and 30 μ g/mL) for 1, 4, 24, and 48 h. After each incubation time, cells were washed and incubated for an additional 24 h in a normal culture condition. Cell viability was assessed using a CellTiter 96 Aqueous One Solution (MTS) Assay (Promega, Madison, WI) according to the manufacturer's protocol. The UV absorbance was measured at 490 nm using a Labsystems Multiskan Plus microplate reader (Labsystems, Finland). Mean cell viabilities were determined relative to a

Table 1. Characterization of PEI–RITC and PEI–RITC-Encapsulated Nanohybrids

formulation	particle size (nm)	zeta potential (mV)	loading ($\mu\text{g}/\text{mg}$ polymer or lipid)	loading efficiency (%)
PEI–RITC	11.2 \pm 5.3	32.1 \pm 2.1		
liposomes	154.2 \pm 13.6	–40.2 \pm 5.7	4.7	94.4
PEG-PLGA NPs	130.2 \pm 9.4	–16.5 \pm 7.0	7.5	75.1
PLGA NPs	117.4 \pm 18.2	–23.6 \pm 13.8	2.2	44.6

negative control (untreated cells). Statistical analysis was performed using OriginPro 8.1 (OriginLab, Northampton, MA). Mean cell viabilities were compared using 1-way ANOVA followed by Tukey's post hoc test at $p < 0.05$.

Cellular Uptake of PEI–RITC-Encapsulated Nanohybrids: Confocal Microscopy Observation. MCF-7 cells were seeded in 4-well chamber slides (Millicell EZ Slide, Millipore, Billerica, MA) at a density of 2.0×10^5 cells/well and incubated in DMEM for 24 h. PEI–RITC (0.5 μg), liposomes (67 μg), PEG-PLGA NPs (242 μg), and PLGA NPs (106 μg) were each dispersed in 1 mL of DMEM to make the concentration of PEI–RITC constant at 0.5 $\mu\text{g}/\text{mL}$ throughout all nanohybrids. Cells were treated with the three nanohybrids and unencapsulated PEI–RITC for 1, 4, 24, and 48 h. Following the treatment, cells were washed with PBS three times, and then 50 μL of Wheat Germ Agglutinin Alexa Fluor 488 conjugate (WGA-AF488, 5 $\mu\text{g}/\text{mL}$, Invitrogen Corporation, Carlsbad, CA) was added to each dish and incubated for 10 min at RT to stain the cell membrane. Cells were washed again with PBS, followed by fixation in 500 μL of 4% paraformaldehyde for 10 min at RT. After washing the excess paraformaldehyde, cells were mounted with antiphotobleaching mounting media with DAPI (Vector Laboratory Inc., Burlingame, CA) and covered with glass coverslips. Cellular uptake was visualized using a Zeiss LSM 510 confocal laser scanning microscope (CLSM, Carl Zeiss, Germany). The 488 nm line of a 30 mW tunable argon laser was used for the excitation of AF488, a 1 mW HeNe at 543 nm for RITC, and a 25 mW diode UV 405 nm laser for DAPI. Emission was filtered at 505–530 nm, 565–595 nm, and 420 nm for AF488, RITC, and DAPI, respectively.

Cellular Uptake of PEI–RITC-Encapsulated Nanohybrids: Flow Cytometry Measurements. MCF-7 cells were seeded in 12-well plates at a density of 1×10^6 cells/well and incubated in DMEM for 24 h. Cells were then treated with unencapsulated PEI–RITC and the three nanohybrids under the same condition described in the cellular uptake experiment. After each incubation period, cells were washed with PBS and then suspended with trypsin/EDTA. Cell suspensions were centrifuged at 3500 rpm for 5 min, resuspended in 500 μL of 1% paraformaldehyde, and transferred to flow cytometry sample tubes. Fluorescence signal intensities from the samples were measured using a MoFlo cell sorter (BD, Franklin Lakes, NJ), and data analysis was performed using Summit v4.3 software (Dako Colorado, Fort Collins, CO).

RESULTS AND DISCUSSION

Preparation and Characterization of PEI–RITC Conjugates and the PEG-PLGA Copolymer. The UV/vis measurements revealed the number of RITC molecules attached to a PEI chain. By constructing a calibration curve of UV absorbance of RITC against various concentrations at 555 nm (λ_{max}), the RITC concentration in a solution of the PEI–RITC conjugate was calculated from the absorbance at 555 nm. The molar ratio of PEI and RITC was then calculated by converting the concentration values to number of moles. The results indicate the presence of

6.2 RITC molecules per PEI chain (Supporting Information Figure S1). Particle size and zeta potential of the conjugates were measured to be 11.2 nm and 32.1 mV, respectively (Table 1). In addition, the chemical structure of PEG–PLGA is confirmed by ^1H NMR as shown in Supporting Information Figure S2. On the basis of the relative integration values of the characteristic peaks of each polymer (see arrows), the ratio of the PEG block to the PLGA block was measured to be 1.3:1–2.4:1.

Preparation and Characterization of PEI–RITC-Encapsulated Nanohybrids. It is highly desirable for a potential tumor-targeted delivery system to possess a size range of less than 200 nm in order to be able to passively accumulate into the tumor tissue. The size of the liposome-based system was controlled by extrusion using a membrane filter with a pore size of 100 nm according to a slightly modified method from a previous report.¹⁶ For encapsulation into the polymeric NPs, the double emulsion method was chosen as it enables encapsulation of hydrophilic materials into a variety of polymers or copolymers with a controlled particle size.^{20,21} As shown in Table 1 and Figure 2, the encapsulation methods employed herein have proven successful in controlling the size, as particle sizes for all three nanohybrids were in the range of 100–150 nm. Both methods also showed relatively good loading efficiencies (45–94%) that correlate well with the reported values.²¹ The zeta potential results suggest that the net surface charges on the NP- and liposome-based nanohybrids are all negative. This is expected since the carboxylic acid groups in PLGA and PEG-PLGA copolymers are deprotonated in neutral pH, and the phospholipid 1,2-dioleoyl-*sn*-glycero-3-phospho-(1'-*rac*-glycerol) (DOPG) is anionic.²² The negative zeta potential values indicate that the encapsulation process in all formulations masked the positive charge on PEI–RITC. The controlled size, along with protection of positive charge from surface exposure, confirmed that we have prepared the nanohybrid systems as designed (Figure 1).

Controlled Release of PEI–RITC-Encapsulated Nanohybrids. Given that our hypothesis of the nanohybrid design is to temporally control cytotoxicity and cellular interactions through controlled release of the PEI conjugates, we first investigated the release kinetics of PEI–RITC from the three nanohybrid systems. The controlled release of PEI–RITC from the nanohybrids was studied by monitoring release profiles in buffers at pH 7.4 and 4.0, as shown in Figure 3. Polymeric NP-based nanohybrids showed slow, sustained release profiles that are typical of degradable polymers, without significant initial burst release. More than one mechanism contributing to drug release from polymeric NPs have been reported, for example, dissolution, surface desorption, diffusion through polymer pores or water-swollen polymer, and surface/bulk erosion of polymer matrix.^{23–25} Although no significant burst release effect was observed, the PEI–RITC release rate from PEG-PLGA and PLGA NPs was faster within the first 24 h, which can be attributed to desorption of PEI–RITC that was located near the surface of the particles. Afterward, the primary mechanism

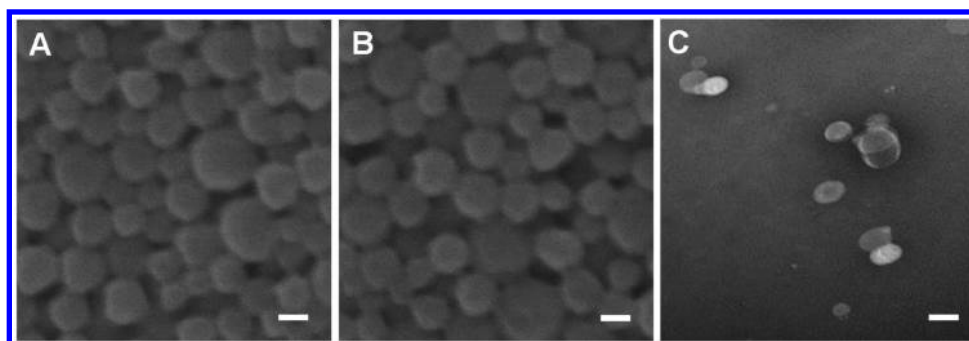


Figure 2. Scanning electron microscopy (SEM) images of (A) PEI–RITC-encapsulated PEG-PLGA NPs and (B) PLGA NPs, scale bar = 100 nm. (C) A transmission electron microscopy (TEM) image of PEI–RITC-encapsulated liposomes, scale bar = 100 nm.

likely becomes diffusion through small channels formed from bulk degradation of the copolymers. PEG-PLGA NPs displayed a higher release rate compared to that of PLGA NPs, attributable to the hydrophilic nature of the PEG block, which facilitates water penetration and subsequent hydrolysis of the polymer.^{26,27} As for the liposomes, release was faster within the first few hours, likely due to PEI–RITC adsorbed on or encapsulated near the liposome surface, followed by a sustained release behavior.²⁸ In addition, PEI–RITC release occurred faster in acidic pH than in pH 7.4 when comparing the same type of nanohybrid system, which is expected since strongly acidic or basic environments can accelerate polymer degradation.²⁹

Kinetically Controlled Cytotoxicity of PEI–RITC-Encapsulated Nanohybrids. Although various mechanisms have been proposed, it is generally accepted that cellular internalization and cytotoxicity of cationic polymers are closely related to each other.^{30–34} One of the proposed mechanisms of toxicity of cationic polymers was described by Hong et al. as being a consequence of nanoscale hole formation in the cell membranes.^{8,9,35,36} The nanoscale pores increased membrane permeability as observed by the leakage of cytosolic enzymes and diffusion of small molecular probes into and out of cells. In this study, we investigated the cytotoxic concentration range of PEI–RITC and the three nanohybrids at extended incubation hours. Figure 4 shows the concentration effect of PEI–RITC and the nanohybrids on the viability of MCF-7 cells as a function of time. At earlier time points (1 and 4 h, Figure 4A and B, respectively), the nanohybrids were significantly less toxic to MCF-7 cells than unencapsulated PEI–RITC, even at high PEI–RITC concentrations of 10–30 $\mu\text{g}/\text{mL}$. Note that it was previously shown that PEI at a concentration of >12 $\mu\text{g}/\text{mL}$ causes significant cell death after 4 h of exposure to the cells.³⁵ This temporal difference in inducing cytotoxicity can indirectly reflect the differences in rates of PEI–RITC release and internalization from those nanohybrids as compared to unencapsulated PEI–RITC. Within the first few hours of incubation, most of the PEI–RITC in the nanohybrids is still entrapped within either polymeric NPs or liposomes, which shield it from direct contact with cell membranes. As the incubation time increases, more PEI–RITC is released, which in turn increases the amount of PEI–RITC in direct contact with cells, rendering them more susceptible to its toxicity. After 48 h of incubation, however, all nanohybrids exhibited similar cytotoxicity (Figure 4D), indicating that PEI–RITC was almost completely released, internalized into the cells, and induced cytotoxicity. Alternatively, this may have been due to the proliferation of residual viable cells, which caused the cytotoxic effects of PEI to even out. Interestingly, among the

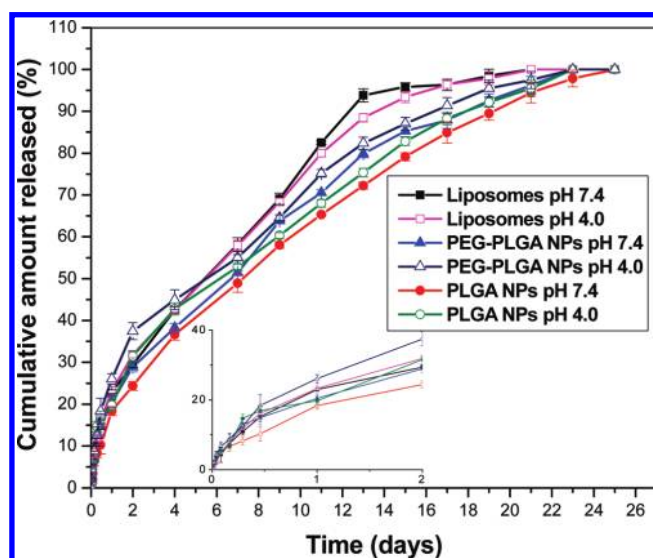


Figure 3. Release profiles of PEI–RITC from the three nanohybrids in PBS buffer with pH 7.4 and acetate buffer with pH 4.0 at 37 °C. Little to no burst release was observed across all nanohybrids, with a sustained release profile up to 23 days. The overall release behavior was faster in pH 4.0 compared to pH 7.4 between the same type of nanohybrid formulation. The inset represents the zoomed-in release profiles for the first 2 days.

three nanohybrids, the liposome-based one showed the most protective effect against PEI–RITC toxicity, particularly after 4 and 24 h (Figure 4B and C). This may be attributed to the difference in the internalization mechanism between liposome- and polymeric NP-based systems since cell internalization of liposomes may occur through endocytosis, membrane fusion, and other mechanisms,¹⁵ allowing them to transfer PEI–RITC without direct contact with the cell membrane.

Kinetic Control over the Cellular Uptake of PEI–RITC-Encapsulated Nanohybrids. Next, we investigated how the controlled release of PEI–RITC and the type of the protective layers (either polymeric NPs or liposomes) affect the rate of cellular uptake of the nanohybrids. Throughout this particular study, a low concentration of PEI–RITC and the three nanohybrid systems was used (0.5 $\mu\text{g}/\text{mL}$ based on PEI–RITC) to ensure that the observations are a result of noncytotoxic interactions between the nanomaterials and cells, as opposed to cell death. As demonstrated in Figure 5, images obtained using confocal laser scanning microscopy (CLSM) qualitatively reveal that the fastest uptake was observed for unencapsulated

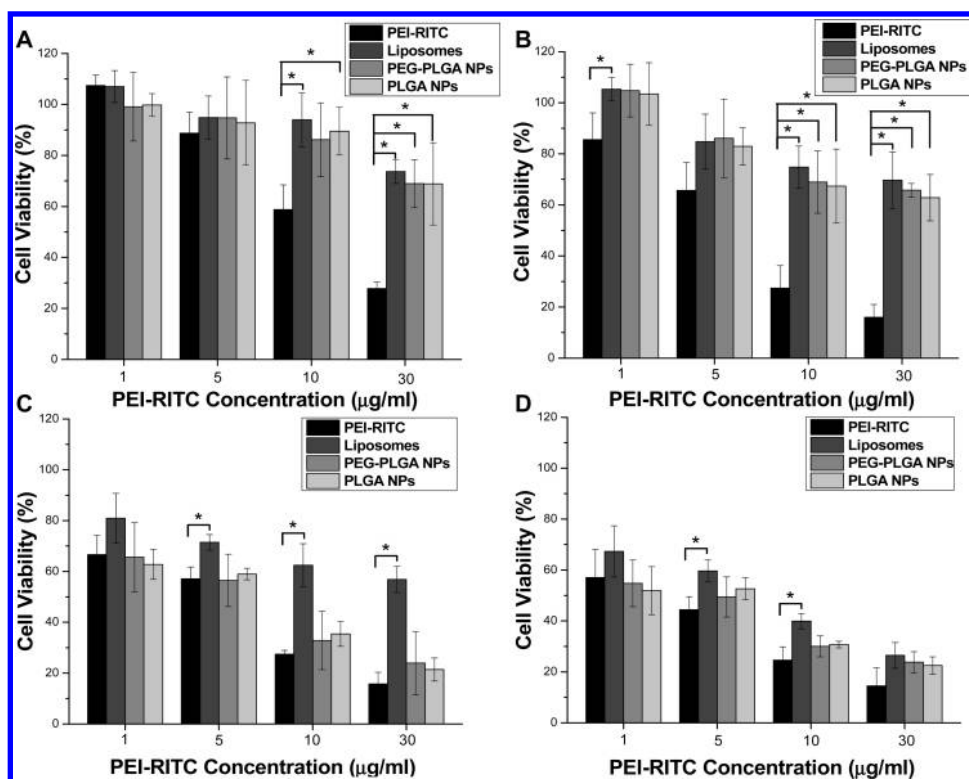


Figure 4. Cytotoxicity of PEI–RITC and the three nanohybrids after incubation with MCF-7 cells for (a) 1 h, (b) 4 h, (c) 24 h, and (d) 48 h. PEI–RITC exhibits cytotoxicity in a concentration and incubation time dependent manner, whereas all nanohybrids show a marked decrease in cytotoxicity kinetics. After 48 h of treatment, all nanohybrids become comparatively toxic to PEI–RITC. * denotes statistical significance ($p < 0.05$) between PEI–RITC and the three nanohybrids, on the basis of a 1-way ANOVA followed by Tukey's post hoc test.

PEI–RITC, followed by, in order of liposomes, PEG–PLGA NPs and PLGA NPs. Red, green, and blue fluorescence channels are, respectively, from PEI–RITC, cell membranes stained by WGA–AF488 conjugate, and nuclei stained by DAPI. The CLSM observation was further supported by quantitative results using a fluorescence activated cell sorter (FACS). As shown in Figure 6, following incubation up to 24 h and in accordance with the CLSM images, the average fluorescence was highest for unencapsulated PEI–RITC, followed by liposomes, PEG–PLGA NPs, and PLGA NPs. After 48 h of incubation, all of the materials (PEI–RITC and the three nanohybrids) displayed similar fluorescence intensities, which is consistent with the cytotoxicity (Figure 4) and confocal data (Figure 5). The fast uptake of PEI is not surprising as PEI is known to spontaneously interact with cells via adsorption on the cell surface and internalization into the cells.³⁵ It has been recently suggested that the biodegradable NPs do not enter cells but rather deliver their cargo via extracellular release or contact-based transfer.^{37,38} This could explain the slow kinetics in PEI–RITC uptake from polymeric NPs observed in this study since the NP-based nanohybrids would have to go through polymer degradation, release, and subsequent internalization of PEI–RITC into the cell. As for the liposome-based nanohybrid system, liposomes exhibited slowest cytotoxicity kinetics (Figure 4) and yet fastest cellular uptake kinetics among the three nanohybrid systems (Figures 5 and 6). This set of observations indicates that, unlike the NP-based nanohybrids, cellular internalization of PEI–RITC upon release is not the only mechanism for cell entry of the liposome-based nanohybrid. In fact, upon adsorption onto the cell surface, it is previously reported that liposomes internalize into the cell through

membrane fusion and/or endocytosis.¹⁵ The coexistence of the internalization mechanisms likely allows relatively fast uptake kinetics with reduced cytotoxicity at early time points. Even though they displayed similar release kinetics in buffer, PLGA NPs had a much slower uptake rate than their PEG–PLGA counterparts. Significant uptake of PLGA NPs was only observed after 24 h, with complete internalization after 48 h. This is again probably due to the hydrophobic nature of the PLGA copolymer, which impedes degradation and subsequent PEI–RITC release.²⁷ The presence of the cellular environment has accentuated the difference between the two types of polymeric NPs, with PEG–PLGA NPs displaying an intermediate uptake rate between the liposome- and PLGA-based nanohybrids. The PEG–PLGA NPs started to show red signals after 4 h of incubation, with complete internalization within 24 h. Although our results indicate that the PEI–RITC internalization from the polymeric NPs largely depends on the degradation and release profiles, it should be noted that other mechanisms such as endocytosis of the whole NPs may coexist.³⁹ As seen in Figure 3, degradation of NP-based nanohybrids may not occur within 2 days, and the red fluorescence observed in the CLSM images (Figure 5) may partially come from the nanoparticles that have been associated with the cells as an intact form. However, it is obvious that the release kinetics in buffer did not follow the same order or rate observed in the cytotoxicity or the cellular uptake studies (Figures 3, 4, and 5). This could be explained by the difference in the microenvironment surrounding the nanohybrids. For the release test shown in Figure 3, all three formulations were suspended in either PBS or acetate buffer only, making the environment markedly different from that in the presence of

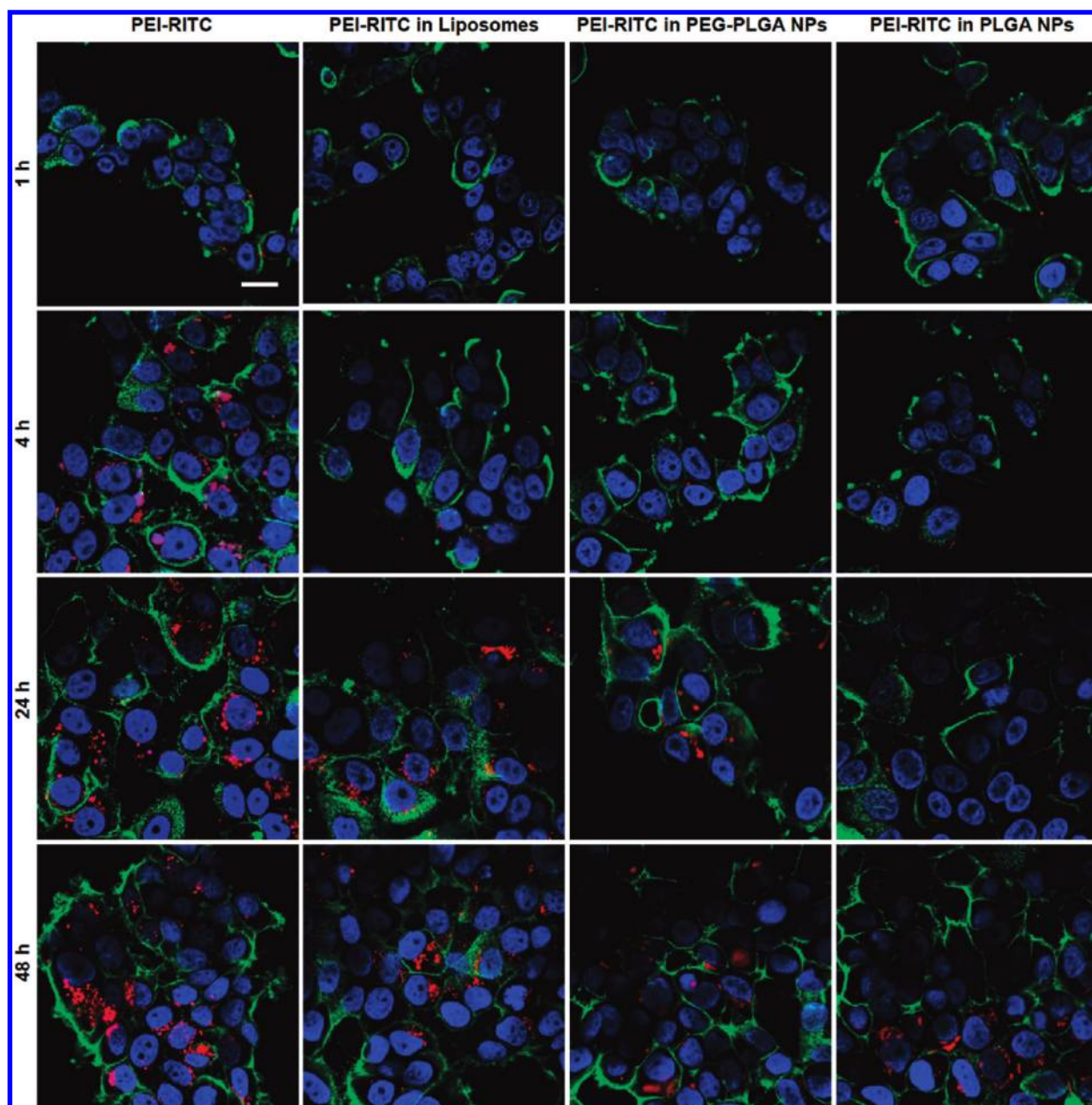


Figure 5. CLSM images of MCF-7 cells following treatment with PEI–RITC and the three nanohybrids (PEI–RITC-encapsulated liposomes, PEG-PLGA NPs, and PLGA NPs) all at a concentration of $0.5 \mu\text{g}/\text{mL}$ based on PEI–RITC for 1 h, 4 h, 24 h, and 48 h (red, PEI–RITC; blue, cell nuclei stained by DAPI; green, cellular membrane stained by WGA-AF 488; scale bar = $20 \mu\text{m}$). Kinetic control over the internalization of PEI–RITC from the three nanohybrid formulations demonstrated as cellular uptake was the second fastest for liposomes compared to unencapsulated PEI–RITC, followed by PEG-PLGA NPs, and last PLGA NPs. The liposome-based and PEG-PLGA NP-based nanohybrids start to internalize into the cells within 4 h, with complete uptake within 24 h. However, the PLGA NP-based nanohybrids do not interact with cell membranes until 4 h of incubation and start to internalize into the cells from the 24 h incubation point.

cells, as in the subsequent cytotoxicity and cell uptake experiments (Figures 4, 5, and 6). Because of the presence of enzymes and proteins, as well as the difference in cellular uptake mechanisms, the differences in release kinetics across the nanohybrids were more accentuated when compared to the release in buffers.

One can argue that our results obtained in the absence of therapeutic agents or genetic materials, i.e., pDNA or siRNA, may not directly represent the biological properties of the nanohybrid systems when used for drug or gene delivery. However, the aim of this preliminary work is to establish kinetic control over cytotoxicity and cellular interactions of PEI. The

results shown in this article reflect the highest possible toxicity of PEI, providing a worst-case scenario in terms of potential toxicity of the delivery system itself. In the case of active drug compounds, which will be covalently linked to the primary amine groups of PEI, we expect the physicochemical and biological behavior of the system to be very similar to what we have described since the presence of RITC molecules on PEI also serves as a model for small molecule drugs. As for complexation with genetic materials, which lowers net positive charges, overall toxicity of PEI would likely be reduced.^{40,41} It is expected that the presence of genetic material will likely affect the overall particle

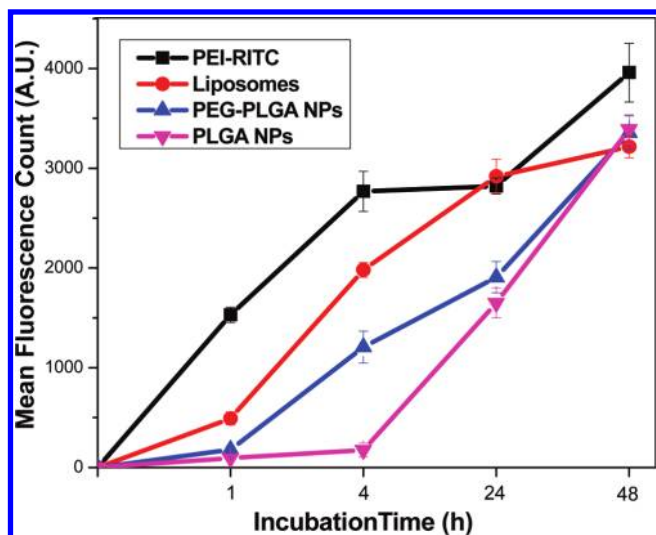


Figure 6. Mean fluorescence following the treatment of MCF-7 cells with PEI-RITC and the three nano hybrids at a concentration of $0.5 \mu\text{g}/\text{mL}$ based on PEI-RITC up to 48 h. Kinetic control over PEI-RITC internalization is further confirmed as unencapsulated PEI-RITC shows the fastest uptake, as indicated by having the highest fluorescence count compared to the three nano hybrid formulations. Cell binding and uptake of the nano hybrids occur in the order of liposomes, PEG-PLGA NPs, and PLGA NPs, which is consistent with the confocal data shown in Figure 5.

size of the nano hybrid systems. However, with proper optimization of the encapsulation process, it is possible to obtain fine control over the size. Furthermore, given that PEI is known to spontaneously interact with cells, facilitating cellular entry,^{35,42,43} it offers an excellent model system for multifunctional vectors without the preparation of complex structures with cytotoxic drugs and targeting agents. Taken together, successful preparation of the three nano hybrid systems (Figure 2 and Table 1), controlled release of encapsulated PEI (Figure 3), kinetically controlled cytotoxicity (Figure 4), and cellular internalization (Figure 5 and 6) all satisfactorily prove that we have successfully achieved the objectives of this study.

CONCLUSIONS

Herein, we report PEI-biodegradable polymer and PEI-liposome nano hybrid delivery systems with particle sizes suitable for passive targeting and with temporally controlled cytotoxicity, release, and cellular uptake kinetics. This work is the first step toward optimization of a new targeted drug delivery system that can be tailored to achieve the desired release and cellular uptake profiles as a platform for controlled drug delivery applications.

ASSOCIATED CONTENT

Supporting Information. UV/vis data for PEI-RITC and ^1H NMR data for PEG-PLGA. This material is available free of charge via the Internet at <http://pubs.acs.org>.

AUTHOR INFORMATION

Corresponding Author

*Department of Biopharmaceutical Sciences, College of Pharmacy, The University of Illinois at Chicago, 833 S. Wood St., Rm 335, Chicago, IL 60612.

ACKNOWLEDGMENT

This work has been partially supported by National Science Foundation (Grant# CBET-0931472) and Vahlteich research award from the University of Illinois College of Pharmacy. S.E.J. was partially supported by a postdoctoral fellowship from National Research Foundation (NRF) of Republic of Korea (Grant # NRF-2009-352-E00066). This work has been conducted in a facility constructed with support from grant C06RR15482 from the NCRR NIH. We thank Drs. Richard Gemeinhart and Hayat Onyuksel for their cooperation in this study, and Dr. Mei Ling Chen from the Research Resource Center at UIC for assistance with confocal microscopy.

REFERENCES

- (1) Nori, A., and Kopecek, J. (2005) Intracellular targeting of polymer-bound drugs for cancer chemotherapy. *Adv. Drug Delivery Rev.* 57, 609–636.
- (2) Patri, A. K., Majoros, I. J., and Baker, J. R. (2002) Dendritic polymer macromolecular carriers for drug delivery. *Curr. Opin. Chem. Biol.* 6, 466–471.
- (3) Verma, I. M., and Somia, N. (1997) Gene therapy - promises, problems and prospects. *Nature* 389, 239–242.
- (4) Bousif, O., Lezoualch, F., Zanta, M. A., Mergny, M. D., Scherman, D., Demeneix, B., and Behr, J. P. (1995) A versatile vector for gene and oligonucleotide transfer into cells in culture and In Vivo - polyethylenimine. *Proc. Natl. Acad. Sci. U.S.A.* 92, 7297–7301.
- (5) Gebhart, C. L., and Kabanov, A. V. (2001) Evaluation of polyplexes as gene transfer agents. *J. Controlled Release* 73, 401–416.
- (6) Akinc, A., Thomas, M., Klivanov, A. M., and Langer, R. (2005) Exploring polyethylenimine-mediated DNA transfection and the proton sponge hypothesis. *J. Gene Med.* 7, 657–663.
- (7) Urban-Klein, B., Werth, S., Abuharbid, S., Czubyko, F., and Aigner, A. (2005) RNAi-mediated gene-targeting through systemic application of polyethylenimine (PEI)-complexed siRNA In Vivo. *Gene Ther.* 12, 461–466.
- (8) Hong, S., Rattan, R., Majoros, I. J., Mullen, D. G., Peters, J. L., Shi, X. Y., Bielinska, A. U., Blanco, L., Orr, B. G., Baker, J. R., and Holl, M. M. B. (2009) The role of ganglioside GM(1) in cellular internalization mechanisms of poly(amidoamine) dendrimers. *Bioconjugate Chem.* 20, 1503–1513.
- (9) Hong, S., Bielinska, A. U., Mecke, A., Keszler, B., Beals, J. L., Shi, X. Y., Balogh, L., Orr, B. G., Baker, J. R., and Holl, M. M. B. (2004) Interaction of poly(amidoamine) dendrimers with supported lipid bilayers and cells: Hole formation and the relation to transport. *Bioconjugate Chem.* 15, 774–782.
- (10) Oupicky, D., Ogris, M., and Seymour, L. W. (2002) Development of long-circulating polyelectrolyte complexes for systemic delivery of genes. *J. Drug Target* 10, 93–98.
- (11) Matsumura, Y., and Maeda, H. (1986) A new concept for macromolecular therapeutics in cancer-chemotherapy: mechanism of tumorotropic accumulation of proteins and the antitumor agent smancs. *Cancer Res.* 46, 6387–6392.
- (12) Yuan, F., Dellian, M., Fukumura, D., Leunig, M., Berk, D. A., Torchilin, V. P., and Jain, R. K. (1995) Vascular permeability in a human tumor xenograft: molecular size dependence and cutoff size. *Cancer Res.* 55, 3752–3756.
- (13) Peer, D., Karp, J. M., Hong, S., FaroKhazad, O. C., Margalit, R., and Langer, R. (2007) Nanocarriers as an emerging platform for cancer therapy. *Nat. Nanotechnol.* 2, 751–760.
- (14) Couvreur, P., and Vauthier, C. (2006) Nanotechnology: Intelligent design to treat complex disease. *Pharm. Res.* 23, 1417–1450.
- (15) Torchilin, V. P. (2005) Recent advances with liposomes as pharmaceutical carriers. *Nat. Rev. Drug Discovery* 4, 145–160.
- (16) Ko, Y. T., Bhattacharya, R., and Bickel, U. (2009) Liposome encapsulated polyethylenimine/ODN polyplexes for brain targeting. *J. Controlled Release* 133, 230–237.

- (17) Kim, I. S., Lee, S. K., Park, Y. M., Lee, Y. B., Shin, S. C., Lee, K. C., and Oh, I. J. (2005) Physicochemical characterization of poly(L-lactic acid) and poly(D,L-lactide-co-glycolide) nanoparticles with polyethylenimine as gene delivery carrier. *Int. J. Pharm.* 298, 255–262.
- (18) Son, S., and Kim, W. J. (2010) Biodegradable nanoparticles modified by branched polyethylenimine for plasmid DNA delivery. *Biomaterials* 31, 134–143.
- (19) Yoo, H. S., and Park, T. G. (2001) Biodegradable polymeric micelles composed of doxorubicin conjugated PLGA-PEG block copolymer. *J. Controlled Release* 70, 63–70.
- (20) Perez, C., Sanchez, A., Putnam, D., Ting, D., Langer, R., and Alonso, M. J. (2001) Poly(lactic acid)-poly(ethylene glycol) nanoparticles as new carriers for the delivery of plasmid DNA. *J. Controlled Release* 75, 211–224.
- (21) Vauthier, C., and Bouchemal, K. (2009) Methods for the preparation and manufacture of polymeric nanoparticles. *Pharm. Res.* 26, 1025–1058.
- (22) Panyam, J., Zhou, W.-Z., Prabha, S., Sahoo, S. K., and Labhasetwar, V. (2002) Rapid endo-lysosomal escape of poly(DL-lactide-co-glycolide) nanoparticles: implications for drug and gene delivery. *FASEB J.* 16, 1217–1226.
- (23) Crotts, G., Sah, H., and Park, T. G. (1997) Adsorption determines in-vitro protein release rate from biodegradable microspheres: Quantitative analysis of surface area during degradation. *J. Controlled Release* 47, 101–111.
- (24) Fu, Y., and Kao, W. J. (2010) Drug release kinetics and transport mechanisms of non-degradable and degradable polymeric delivery systems. *Expert Opin. Drug Delivery* 7, 429–444.
- (25) Polakovic, M., Gorner, T., Gref, R., and Dellacherie, E. (1999) Lidocaine loaded biodegradable nanospheres II. Modelling of drug release. *J. Controlled Release* 60, 169–177.
- (26) Penco, M., Marcioni, S., Ferruti, P., D'Antone, S., and Deghenghi, R. (1996) Degradation behaviour of block copolymers containing poly(lactic-glycolic acid) and poly(ethylene glycol) segments. *Biomaterials* 17, 1583–1590.
- (27) Avgoustakis, K., Beletsi, A., Panagi, Z., Klepetsanis, P., Karydas, A. G., and Ithakissios, D. S. (2002) PLGA-mPEG nanoparticles of cisplatin: in vitro nanoparticle degradation, in vitro drug release and In Vivo drug residence in blood properties. *J. Controlled Release* 79, 123–135.
- (28) Atyabi, F., Farkhondehfai, A., Esmaili, F., and Dinarvand, R. (2009) Preparation of pegylated nano-liposomal formulation containing SN-38: In vitro characterization and In Vivo biodistribution in mice. *Acta Pharm. (Zagreb, Croatia)* 59, 133–144.
- (29) Faisant, N., Akiki, J., Siepmann, F., Benoit, J. P., and Siepmann, J. (2006) Effects of the type of release medium on drug release from PLGA-based microparticles: Experiment and theory. *Int. J. Pharm.* 314, 189–197.
- (30) Jevprasesphant, R., Penny, J., Attwood, D., and D'Emanuele, A. (2004) Transport of dendrimer nanocarriers through epithelial cells via the transcellular route. *J. Controlled Release* 97, 259–267.
- (31) Kopatz, I., Remy, J. S., and Behr, J. P. (2004) A model for non-viral gene delivery: through syndecan adhesion molecules and powered by actin. *J. Gene Med.* 6, 769–776.
- (32) Manunta, M., Nichols, B. J., Tan, P. H., Sagoo, P., Harper, J., and George, A. J. T. (2006) Gene delivery by dendrimers operates via different pathways in different cells, but is enhanced by the presence of caveolin. *J. Immunol. Methods* 314, 134–146.
- (33) Seib, F. P., Jones, A. T., and Duncan, R. (2007) Comparison of the endocytic properties of linear and branched PEIs, and cationic PAMAM dendrimers in B16f10 melanoma cells. *J. Controlled Release* 117, 291–300.
- (34) Kitchens, K. M., Kolhatkar, I. B., Swaan, P. W., and Ghandehari, H. (2008) Endocytosis inhibitors prevent poly(amidoamine) dendrimer internalization and permeability across Caco-2 cells. *Mol. Pharmaceutics* 5, 364–369.
- (35) Hong, S., Leroueil, P. R., Janus, E. K., Peters, J. L., Kober, M. M., Islam, M. T., Orr, B. G., Baker, J. R., and Holl, M. M. B. (2006) Interaction of polycationic polymers with supported lipid bilayers and cells: Nanoscale hole formation and enhanced membrane permeability. *Bioconjugate Chem.* 17, 728–734.
- (36) Leroueil, P. R., Hong, S., Mecke, A., Baker, J. R., Orr, B. G., and Holl, M. M. B. (2007) Nanoparticle interaction with biological membranes: Does nanotechnology present a janus face? *Acc. Chem. Res.* 40, 335–342.
- (37) Chen, H., Kim, S., Li, L., Wang, S., Park, K., and Cheng, J.-X. (2008) Release of hydrophobic molecules from polymer micelles into cell membranes revealed by Forster resonance energy transfer imaging. *Proc. Natl. Acad. Sci. U.S.A.* 105, 6596–6601.
- (38) Xu, P. S., Gullotti, E., Tong, L., Highley, C. B., Errabelli, D. R., Hasan, T., Cheng, J. X., Kohane, D. S., and Yeo, Y. (2009) Intracellular drug delivery by poly(lactic-co-glycolic acid) nanoparticles, revisited. *Mol. Pharmaceutics* 6, 190–201.
- (39) Vasir, J. K., and Labhasetwar, V. (2007) Biodegradable nanoparticles for cytosolic delivery of therapeutics. *Adv. Drug Delivery Rev.* 59, 718–728.
- (40) Kunath, K., von Harpe, A., Fischer, D., Peterson, H., Bickel, U., Voigt, K., and Kissel, T. (2003) Low-molecular-weight polyethylenimine as a non-viral vector for DNA delivery: comparison of physicochemical properties, transfection efficiency and In Vivo distribution with high-molecular-weight polyethylenimine. *J. Controlled Release* 89, 113–125.
- (41) Zhao, Q. Q., Chen, J. L., Lv, T. F., He, C. X., Tang, G. P., Liang, W. Q., Tabata, Y., and Gao, J. Q. (2009) N/P ratio significantly influences the transfection efficiency and cytotoxicity of a polyethylenimine/chitosan/DNA complex. *Biol. Pharm. Bull.* 32, 706–710.
- (42) Neu, M., Fischer, D., and Kissel, T. (2005) Recent advances in rational gene transfer vector design based on poly(ethylene imine) and its derivatives. *J. Gene Med.* 7, 992–1009.
- (43) Fischer, D., Li, Y. X., Ahlemeyer, B., Kriegelstein, J., and Kissel, T. (2003) In vitro cytotoxicity testing of polycations: influence of polymer structure on cell viability and hemolysis. *Biomaterials* 24, 1121–1131.